Available online at www.sciencedirect.com
ScienceDirect
Pattern Recognition Letters 29 (2008) 1007–1020
Pattern Recognition Letters
www.elsevier.com/locate/patrec

Fuzzy-based algorithm for color recognition of license plates

Feng Wang [a,*], Lichun Man [b], Bangping Wang [a], Yijun Xiao [a], Wei Pan [a], Xiaochun Lu [a]

[a] Institute of Image and Graphics, School of Computer Science, Sichuan University, Chengdu 610064, Sichuan, PR China
[b] Department of Computer Science, Zhongyuan University of Technology, Zhengzhou 450007, Henan, PR China

Received 5 April 2007; received in revised form 25 October 2007
Available online 9 February 2008

Communicated by H.H.S. Ip

Abstract

Color recognition of license plates plays an important role in a license plate recognition (LPR) system. But it can be a challenging task as the appearances of license plates are affected by various factors such as illumination, camera characteristics, etc. And the color features of license plates in different places may be quite different. To address these concerns, this paper presents an algorithm based on fuzzy logic. The HSV (hue, saturation and value) color space is employed to perform color feature extraction. Three components of the HSV space are firstly mapped to fuzzy sets according to different membership functions. The fuzzy classification function for color recognition is, then, described by the fusion of three weighted membership degrees. For adaptation of the proposed algorithm, we also present a learning algorithm to obtain the correlative parameters. On a DSP-based embedded LPR platform, comparisons were drawn with other classifiers within three sets of test images. Experimental results show that the proposed algorithm achieves higher classification accuracy and better adaptability.

Keywords: Color recognition; Fuzzy logic; HSV color space; License plate recognition (LPR)

1. Introduction

LPR is one of the key technologies of Intelligent Transportation System (ITS). It has been widely used in many systems, such as road traffic monitoring, parking lots access control, highway electronic toll collection, red-light violation enforcement, finding stolen cars, gathering traffic flow statistics and so on. Color recognition of license plates is an important step in LPR system. In Mainland China, there are mainly four kinds of vehicle license plates, i.e. blue, black, yellow and white. And their purposes are different: blue is for civilian vehicles, black for foreign institution, diplomatic, Hong Kong and Macao vehicles, yellow for trucks and buses while white for police, military and some civilian vehicles. On the one hand, two license plates with the same characters but different colors do not mean the same one. On the other hand, we can find from Fig. 1 that different license plates may have different formats, while the type of a license plate is identified by its color. Therefore, color recognition has a great influence on the subsequent steps, e.g. character separation. So accuracy improvement of color recognition is helpful to improve the final recognition accuracy of license plates.

Extensive work about color has been proposed. Color histogram (Swain and Ballard, 1991), color moments (Stricker and Orengo, 1995), color correlogram (Huang et al., 1997), color set (Smith and Chang, 1997), etc. are utilized as important color features for image matching and retrieval. To decrease the influence of illumination, color constancy (Funt and Finlayson, 1995; Tsin et al., 2001), normalization (Finlayson and Xu, 2003; Lin et al., 2002) and other schemes (Berwick and Lee, 2004; Drew et al., 1998) are proposed. But their applicability to realistic outdoor images still needs establishing (Buluswar and Draper, 1998). Some studies perform color recognition task by the

* Corresponding author. Tel.: +86 28 85417865; fax: +86 28 85372688.
E-mail address: wangfeng_scu@yahoo.com.cn (F. Wang).

0167-8655/$ - see front matter © 2008 Elsevier B.V. All rights reserved.
doi:10.1016/j.patrec.2008.01.026

Fig. 1. Main vehicle license plate types in Mainland China: (a) blue; (b) black (foreign institution); (c) black (consulate); (d) black (Hong Kong); (e) black (Macao); (f) yellow (installed in the front of vehicles); (g) white (armed police); (h) white (military); (i) white (police); (j) white (military); (k) white (civilian) and (l) yellow (installed at the back of vehicles).

methods of optical processing (Chen and Wu, 2005; Parkkinen et al., 1988) and hardware chip (Geske et al., 2003). They are lack of general availability because of the specific instrument.

With respect to color spaces, some literatures are based on the RGB (red, green and blue) color space (Lalanne and Lempereur, 1998; Stachowicz and Lemke, 2000; Xu et al., 2003; Yang et al., 2005; Zhai et al., 2005). But RGB is a linear color space where three components are highly correlative. And it is very sensitive to lightness and shading (Gevers and Smeulders, 1999; Lin et al., 2002; Tao and Xu, 2001). To overcome the problem, the standard RGB color space is usually converted into normalized RGB space: *rgb* (Lalanne and Lempereur, 1998; Buluswar and Draper, 1998). But it is not appropriate with the presence of highlights (Gevers and Smeulders, 1999). Buluswar and Draper (1998) also predicted the colors of objects through context-based models of daylight illumination and hybrid surface reflectance. However, considering fantasticality of the natural environment, it is difficult to build a sample library or environment models that cover all kinds of lighting conditions. And it will increase the computational cost too. In addition, it is notable that RGB values in machine vision are different from those in human perception. Because human eyes distinguish objects with brightness, hue and saturation of colors, they cannot determine color features from RGB values directly (Tao and Xu, 2001). Therefore, the RGB color space is not effective to perform color comparison in natural environment. Some other researchers employed nonlinear color space, such as HSI, HSV and CIELAB, to accomplish object identification or image retrieval task (Fu et al., 2004; Pavlova et al., 1996; Vertan and Boujemaa, 2000; Wang et al., 2004; Yang and Wang, 2004). But some methods worked under restricted and supervised conditions while some methods could not meet the real-time requirement of LPR. In the practical LPR application environment, however, color distortion can be caused by many reasons (Buluswar and Draper, 1998), such as too strong lighting of vehicles at night, degrading of license plates and imaging parameters and so on. In some cases, even the color distinction between black and blue, yellow and white are not obvious for a human observer. Fig. 2 gives such examples that are easy to be mixed up. Furthermore, the color features of

Fig. 2. License plates whose colors are easy to be mixed up: (a) blue; (b) black; (c) yellow and (d) white.

license plates in different places may be quite different. Fig. 3 shows some images of blue plates under different conditions and places.

In addition, some of the past studies adopted thresholds and rules determination method (Fu et al., 2004; Wang et al., 2004; Yang and Wang, 2004). It is only suitable for those images with high qualities or under specific conditions. Once conditions change, the perceived color of an object can vary significantly, thus making color recognition difficult. In order to improve the recognition accuracy, more rules and thresholds have to be added manually. However, it is tedious and difficult to establish these thresholds and rules. They are lacking in adaptability too. In order to adapt to the practical situation in different places, these rules and thresholds need re-establishing, bringing lots of troubles to practical applications.

From the above analysis, it is clear that color recognition of license plates is uncertain because of many factors. Fuzzy mathematics is a valid method to solve uncertain problems in real scenes. Therefore, a fuzzy-based algorithm for color recognition of license plates is presented in this paper. We adopt the HSV color space to implement color recognition, because of its similarity with the way human observes colors (Tao and Xu, 2001; Vitabile et al., 2001). Fuzzy logic is introduced to improve the recognition accuracy. The correlative thresholds and weights are obtained from a learning algorithm, thus improving the adaptability of the proposed algorithm. Experiments are conducted on a DSP-based embedded LPR platform, compared with some other approaches. The experimental results demonstrate that both recognition accuracy and execution time can meet the requirements of the practical engineering applications.

The rest of the paper is organized as follows: Section 2 describes the implementation of the proposed algorithm in detail, including obtainment of valid license plate regions, reverse color identification, color space conversion, and fuzzy color recognition, etc. The experimental results and discussions are provided in Section 3. And finally we conclude this paper in Section 4.

2. Implementation of the proposed algorithm

The flowchart of the proposed algorithm is shown in Fig. 4.

2.1. Color feature extraction

The first step in color recognition of license plates is to perform color feature extraction. It consists of obtainment of valid license plate regions, reverse color identification and color space conversion.

2.1.1. Obtainment of valid license plate regions

Let I denote an original vehicle image to be recognized. To obtain the approximate location of I's license plate, we firstly perform the following operations:

(1) Accomplish noise elimination and other data preprocessing operations on I.
(2) According to texture information of horizontal and vertical edge images (edge detection method is used to locate the candidate license plates in our system), obtain some candidate rectangle regions.
(3) Based on size, histogram distribution and other information, filter some invalid rectangle regions, e.g. English brands, radiators and vehicle lights. Then obtain the top N_p (N_p is set to 3 in our system) regions by the rank of confidence levels.
(4) Perform geometric corrections and obtain the candidate license plate regions.

This is a rough localization process, so it cannot always obtain the precise location of the license plate.

Fig. 3. Blue plates under different conditions and places.

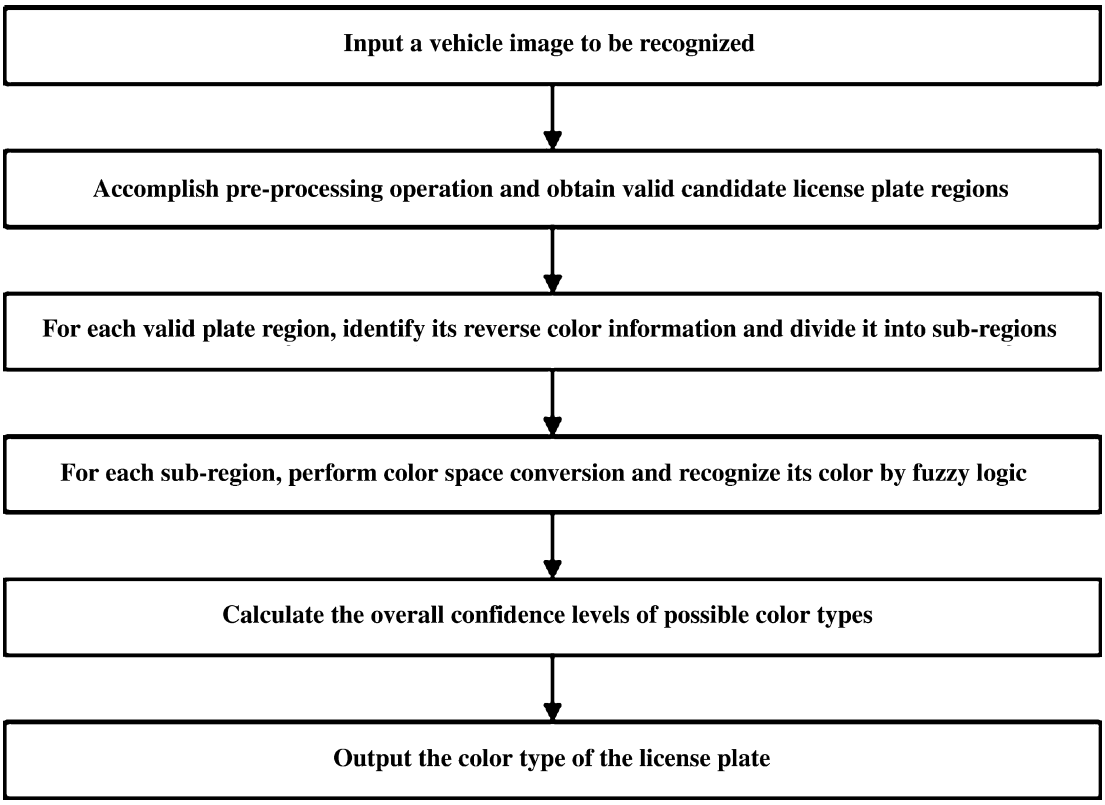

Fig. 4. Flowchart of the proposed algorithm.

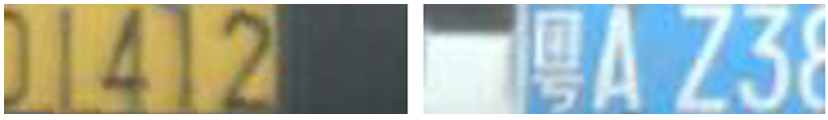

Fig. 5. Candidate license plate regions that exist invalid areas after rough localization.

Fig. 5 gives such two examples that include invalid areas. After the color of the license plate is identified, the approximate coordinates can be adjusted in the subsequent steps to obtain the precise location. In order to decrease the influence of invalid areas on color recognition, we need to obtain the valid license plate region.

For convenience, let $R=(L_R, T_R, R_R, B_R)$ represent a rectangle region R, where (L_R, T_R) and (R_R, B_R) denote, respectively, the coordinates of top left corner and bottom right corner. In our DSP-based embedded LPR system, we adopt the following steps to obtain a valid license plate region, considering real-time requirement:

(1) Extend a candidate character region to obtain a rectangle region (R_t), which is much wider than the real license plate region. Let $M^x_{R_t}$ be the abscissa of R_t's center point. Then identify the relative position of the license plate, i.e. on the left side or right side relative to the center of R_t

$$S_l = \sum_{i=M^x_{R_t}-L}^{M^x_{R_t}} \sum_{j=T_{R_t}}^{B_{R_t}} P_h[i][j], \tag{1}$$

$$S_r = \sum_{i=M^x_{R_t}}^{M^x_{R_t}+L} \sum_{j=T_{R_t}}^{B_{R_t}} P_h[i][j], \tag{2}$$

$$X_l = \begin{cases} 1, & \text{if } (S_l > S_r), \\ 0, & \text{otherwise}, \end{cases} \tag{3}$$

where L is an experience value (L is set to 80 in our system), P_h is the horizontal edge image of I, and $P_h[\cdot][\cdot]$ denotes the value of a pixel in P_h. Eqs. (1) and (2) calculate, respectively, the sum of gray scale difference of the left and right halves. According to the statistical information, Eq. (3) identifies the relative position of the license plate, where 1 means that the plate is on the left side and 0 means the right side. If S_l is greater than S_r, it means that the texture feature of the left side is more obvious than that of the right side and vice versa.

(2) Obtain the candidate plate rectangle region R_c

$$R_c = \begin{cases} (\max(M^x_{R_t} - \theta, 0), T_{R_t}, M^x_{R_t}, B_{R_t}), & \text{if}(X_1 = 1), \\ (M^x_{R_t}, T_{R_t}, \min(M^x_{R_t} + \theta, w_I - 1), B_{R_t}), & \text{otherwise}, \end{cases} \tag{4}$$

where max and min operators select, respectively, the maximum and minimum values of the operand, and w_I is the width of image I. According to the license plate's relative position, Eq. (4) obtains the candidate license plate region by extending θ (experience value) pixels from R_t's center to left or right.

(3) Obtain the valid license plate region R_v

$$d = ||\overline{G_m} - \overline{G_l}| - |\overline{G_m} - \overline{G_r}||, \tag{5}$$

$$R_v = \begin{cases} R^r_c, & \text{if } (d \geqslant T_g) \text{ and } (X_1 = 1), \\ R^l_c, & \text{if } (d \geqslant T_g) \text{ and } (X_1 = 0), \\ R_c, & \text{otherwise}. \end{cases} \tag{6}$$

R_c is equally divided into three parts, i.e. left, middle and right. Let $\overline{G_l}$, $\overline{G_m}$ and $\overline{G_r}$ denote, respectively, the mean values of the three parts in P_h. Eq. (5) calculates their difference information d. If d exceeds a pre-defined threshold T_g, we assume that there exists an invalid area in R_c. According to the license plate's relative position, Eq. (6) chooses the right 2/3 parts (R^r_c) or the left 2/3 parts (R^l_c) of R_c to be the valid license plate region.

Fig. 6 shows the process of obtaining a valid license plate region. For processing convenience, we define another image that is larger than the input one and the gray scale of each pixel is set to 0. The image to be processed is put at the center of the larger one. For display convenience, the redundant parts of (b) and (c) in Fig. 6 are removed here.

2.1.2. Reverse color identification

To extract the color feature of a valid license plate region, its background must be firstly obtained. This task can be accomplished by analyzing the relationship between the average gray level and the gray levels of pixels in a gray image of license plate.

When color images of four kinds of license plates are converted into gray images, the features of blue and black plates are different from those of yellow and white plates, as shown in Fig. 7.

From Fig. 7, it is clear that the gray images of blue and black plates are white character with black background while the gray images of yellow and white plates are the opposite. Therefore, for the gray images of blue and black plates, the pixels whose gray levels are less than the average gray level belong to the background. For yellow and white plates, it is the opposite situation.

For convenience, it is necessary to identify whether a license plate region needs reverse color processing or not. Let A_g be the average gray level of a rectangle region. Let N_b and N_s denote, respectively, the number of pixels whose gray levels are greater and less than A_g. Then we define

$$\xi = \begin{cases} 1, & \text{if } (N_b > N_s), \\ 0, & \text{otherwise}. \end{cases} \tag{7}$$

In our system, yellow and white plates are regarded as needing to perform reverse color processing, i.e. $\xi = 1$, vice versa. In this way, we can divide four types of license plates into two classes, i.e. class blue/black and class yellow/white. Then we can just identify that a license plate is blue or black, yellow or white. Thus, the 4-class problem is converted into two 2-class problems, increasing the recognition efficiency.

2.1.3. Color space conversion

After the background of a valid license plate region is obtained, color space conversion is the final step in color feature extraction. Because the format of a captured image in our system is YUV 422, it has to be converted into the HSV space.

Let small capital letters y, u, and v' denote, respectively, the luminance (or luma) signal and two chrominance signals of YUV data. Let small capital letters r, g and b denote, respectively, three components of the RGB color space. The values of y, u, v', r, g and b are all kept in the $[0, 255]$ range. Let small capital letters h, s and v denote, respectively, three channels of the HSV color space.

For a background region, its average YUV values are firstly converted into RGB values, according to the equations given by Julien (http://www.fourcc.org/fccyvrgb.php).

$$r = y + 1.402(v' - 128), \tag{8}$$

$$g = y - 0.34414(u - 128) - 0.71414(v' - 128), \tag{9}$$

$$b = y + 1.772(u - 128). \tag{10}$$

Based on the work of Makoto and Yasuhiro (1988), they are then converted into the HSV color space. Let the number of hue be 60. Let $I_{\max} = \max(r, g, b)$, $I_{\min} = \min(r, g, b)$ and $\delta = I_{\max} - I_{\min}$. Then the transformation from RGB to HSV can be described by the following equations:

$$s = \begin{cases} 0, & \text{if}(I_{\max} = 0), \\ \frac{\delta}{I_{\max}} \times 255, & \text{otherwise}, \end{cases} \tag{11}$$

$$v = I_{\max} \tag{12}$$

and

$$h = \begin{cases} \text{undefined}, & \text{if } (s = 0), \\ \frac{g-b}{\delta} \times 60, & \text{if } (s \neq 0) \text{ and } (I_{\max} = r) \text{ and } (g \geqslant b), \\ \frac{g-b}{\delta} \times 60 + 360, & \text{if } (s \neq 0) \text{ and } (I_{\max} = r) \text{ and } (g < b), \\ \left[2 + \frac{b-r}{\delta}\right] \times 60, & \text{if } (s \neq 0) \text{ and } (I_{\max} = g), \\ \left[4 + \frac{r-g}{\delta}\right] \times 60, & \text{if } (s \neq 0) \text{ and } (I_{\max} = b). \end{cases} \tag{13}$$

Obviously, value ranges of the three components in the HSV color space are $h \in [0, 360)$, $s \in [0, 255]$ and $v \in [0, 255]$, respectively.

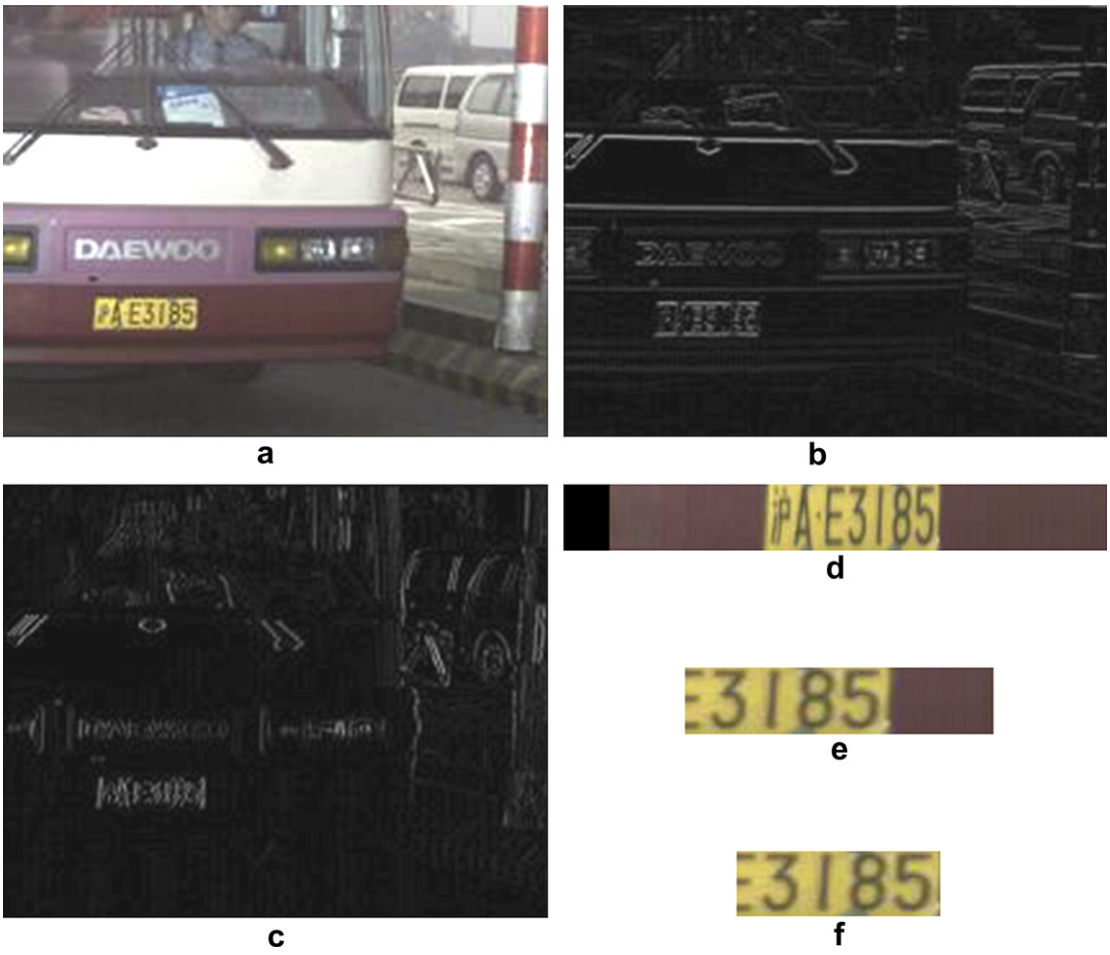

Fig. 6. Process of obtaining a valid license plate region: (a) original vehicle image; (b) horizontal edge image; (c) vertical edge image; (d) rectangle region extended from the candidate character region; (e) candidate license plate region and (f) valid license plate region.

Fig. 7. Color images of four kinds of license plates and the corresponding gray images: (a) color image of blue plate; (b) gray image of blue plate; (c) color image of black plate; (d) gray image of black plate; (e) color image of yellow plate; (f) gray image of yellow plate; (g) color image of white plate and (h) gray image of white plate.

2.2. Fuzzy color recognition

Once the HSV color feature of a valid license plate region is extracted, the color recognition task can then be performed. Since the captured vehicle image is not perfect, uncertainties should be taken into account during color recognition of license plates. Fuzzy logic is introduced here to improve the recognition performance.

Let $U = \{(h,s,v)|h \in [0,360), s,v \in [0,255]\}$, where h, s and v denote hue, saturation and value, respectively. Let $F(U)$ denote the fuzzy representation of colors in the HSV space. It is a fuzzy set on U and is defined by Eq. (20) in Section 2.2.1. We first define membership functions to implement fuzzy maps.

2.2.1. Fuzzy maps

In order to express fuzzy degrees of three components in the HSV color space, we establish the following membership functions, according to the analysis of many experimental results:

(1) Membership function of hue for class blue/black:

$$A_{\tilde{h}0}(h) = \begin{cases} h/200, & 0 \leqslant h < 200, \\ 1, & 200 \leqslant h \leqslant 270, \\ (360-h)/90, & 270 < h < 360. \end{cases} \tag{14}$$

(2) Membership function of hue for class yellow/white:

$$A_{\tilde{h}1}(h) = \begin{cases} (h/30)^2, & 0 \leqslant h < 30, \\ 1, & 30 \leqslant h \leqslant 90, \\ ((360-h)/270)^2, & 90 < h < 360. \end{cases} \tag{15}$$

(3) Membership function of saturation for class blue/black:

$$A_{\tilde{s}0}(s) = \begin{cases} s/p_{s0}, & 0 \leqslant s < p_{s0}, \\ 1, & p_{s0} \leqslant s \leqslant 255. \end{cases} \tag{16}$$

(4) Membership function of saturation for class yellow/white:

$$A_{\tilde{s}1}(s) = \begin{cases} (s/p_{s1})^2, & 0 \leqslant s < p_{s1}, \\ 1, & p_{s1} \leqslant s \leqslant 255. \end{cases} \tag{17}$$

(5) Membership function of value for class blue/black:

$$A_{\tilde{v}0}(v) = \begin{cases} v/p_{v0}, & 0 \leqslant v < p_{v0}, \\ 1, & p_{v0} \leqslant v \leqslant 255. \end{cases} \tag{18}$$

(6) Membership function of value for class yellow/white:

$$A_{\tilde{v}1}(v) = \begin{cases} (v/p_{v1})^2, & 0 \leqslant v < p_{v1}, \\ 1, & p_{v1} \leqslant v \leqslant 255. \end{cases} \tag{19}$$

For computational similarity, we use trapezia distributions (Eqs. (14), (16) and (18)) and second-degree parabola distributions (Eqs. (15), (17) and (19)) to describe, respectively, the fuzzy distributions of three HSV components for class blue/black and class yellow/white. Because colors in the HSV space are fairly consistent with human perception and the hue component is invariant to illumination and shading, the peaks of hue membership functions (Eqs. (14) and (15)) are defined directly according to how people experience colors. While the peaks of saturation and value membership functions (Eqs. (16)–(19)) are set to parameters which need to learn from training samples. In Eqs. (16)–(19), saturation thresholds p_{s0}, p_{s1} and value thresholds p_{v0}, p_{v1} are all kept in the $[0,255]$ range. Based on these membership functions, fuzzy membership degrees of three HSV components can be calculated.

According to the reverse color information obtained from Section 2.1.2, we can choose different membership functions to implement fuzzy maps on the respective sets of hue, saturation and value. And each of them provides partial information for recognizing the color of a license plate. But their contributions may be different. To express the fuzzy representation of colors, the three fuzzy maps are then linearly combined into a single map by

$$F(c) = \sum_{i=1}^{3} w_i \times m_i, \tag{20}$$

where c is a color vector ($c \in U$), $w_i, m_i \in [0,1]$ and $\sum_{i=1}^{3} w_i = 1$. The variables m_1, m_2 and m_3 represent, respectively, the membership degrees of hue, saturation and value, which can be calculated by Eqs. (14)–(19). And w_1, w_2 and w_3 are weights reflecting the relative degrees of importance among the corresponding fuzzy maps. Eq. (20) also acts as the fuzzy classification function for class blue/black and class yellow/white. Based on Eq. (20), the color recognition result can be drawn according to threshold principle, which will be detailed in Section 2.2.2.

To improve adaptability, the above parameters (saturation and value thresholds, weights and classification thresholds) are learned from training samples by a learning algorithm. Based on the learning results, they can also be adjusted easily according to the practical situation. For class blue/black and class yellow/white, the learning algorithm is described as follows:

(1) Obtain the hybrid mean values of saturation and value from training samples.
(2) Obtain the value ranges of saturation and value from training samples. Then re-perform step (3) and step (4).
(3) According to the classification error minimization inductive principle, obtain the thresholds of saturation and value membership functions, such that the distances between current parameters and the hybrid mean values obtained from step (1) are minimized.
(4) Based on the classification error minimization principle, obtain the weights and classification threshold, such that the distance between weights of saturation and value is maximized while weight of hue is minimized.
(5) Output the learned parameters.

2.2.2. Color recognition

In order to improve the accuracy of color recognition, a valid license plate region is divided into some sub-regions with the same size. After each sub-region's color is recognized based on fuzzy logic, the final result can then be identified. The computational complexity of the color recognition process is $O(W \times H)$, where W and H are, respectively, the width and height of the valid license plate region obtained from Section 2.1.1.

For convenience, let $c_k \in U(1 \leqslant k \leqslant N_z)$, where N_z refers to the number of sub-regions to divide the valid license plate region R_v. Let R_k represent a small rectangle region, which corresponds to a sub-region after performing multi-region division on R_v. And R_k's color feature vector is represented by c_k. Let $x \in \{0,1,2,3\}$ be the class label of four standard types of license plates, i.e. blue, black, yellow and white. Let H_R and W_R represent the height and width of a rectangle region R, respectively. And we just use the relative coordinates of a region in this section.

For each sub-region, we first obtain its background. According to the analysis in Section 2.1.2, we have the following equations:

$$\overline{A_y} = \frac{1}{W_{R_v} \times H_{R_v}} \sum_{i=0}^{W_{R_v}-1} \sum_{j=0}^{H_{R_v}-1} R_v^y[i][j], \tag{21}$$

$$Z_k = \begin{cases} \sum_{i=0}^{W_{R_k}-1} \sum_{j=0}^{H_{R_k}-1} f_{yw}(R_k^y[i][j]), & \text{if } (\xi = 1), \\ \sum_{i=0}^{W_{R_k}-1} \sum_{j=0}^{H_{R_k}-1} f_{bb}(R_k^y[i][j]), & \text{otherwise}, \end{cases} \tag{22}$$

where

$$f_{yw}(p) = \begin{cases} 1, & \text{if } (\xi = 1) \text{ and } (p_y > \overline{A_y}), \\ 0, & \text{otherwise}, \end{cases} \tag{23}$$

$$f_{bb}(p) = \begin{cases} 1, & \text{if } (\xi = 0) \text{ and } (p_y < \overline{A_y}), \\ 0, & \text{otherwise}. \end{cases} \tag{24}$$

Eq. (21) calculates the average gray scale of R_v, where $R_v^y[\cdot][\cdot]$ is the gray scale, i.e. Y (luminance or luma) information of YUV data, of a pixel. Eq. (22) obtains the confidence level of R_k's falling into class yellow/white or class blue/black, which is represented by the number of background pixels of R_k. Eqs. (23) and (24) identify that a pixel, p, belongs to character or background of a license plate, where p_y is the gray scale of p, 1 and 0 denote background and character, respectively.

To extract the color feature of R_k, we first calculate the mean values of y, u and v', i.e. $(\bar{y}, \bar{u}, \overline{v'})$, according to Eq. (25):

$$\overline{f} = \frac{1}{Z_k} \sum_{i=0}^{W_{R_k}-1} \sum_{j=0}^{H_{R_k}-1} R_k^f[i][j], \quad f \in \{y, u, v'\}. \tag{25}$$

Eq. (25) subjects to $f_{yw}(R_k^y[i][j]) = 1$ or $f_{bb}(R_k^y[i][j]) = 1$, namely the pixel must belong to the background of R_k. Next we convert $(\bar{y}, \bar{u}, \overline{v'})$ into the HSV color space and obtain the corresponding color feature vector $(\bar{h}, \bar{s}, \bar{v})$, as detailed in Section 2.1.3. Thus the color feature of R_k can be represented by $c_k = (\bar{h}, \bar{s}, \bar{v})$. According to Eqs. (14)–(19), the membership degrees of c_k's three components can be calculated. Then the membership degree, $F(c_k)$, of its falling into a certain color is obtained by Eq. (20). The final conclusion of c_k can be expressed as

$$I_c(c_k) = \begin{cases} I_{c0}(c_k), & \text{if } (\xi = 0), \\ I_{c1}(c_k), & \text{otherwise}, \end{cases} \tag{26}$$

where $I_{c0}(c_k)$ and $I_{c1}(c_k)$ identify, respectively, c_k's color type between blue and black as well as yellow and white, according to the reverse color information. And their classification rules are described by Eqs. (27) and (28), respectively.

$$I_{c0}(c_k) = \begin{cases} 0, & \text{if } (F(c_k) \geqslant T_0) \\ & \quad \text{or } ((K_0 = 1) \text{ and } (A_{\underset{h0}{\sim}}(\bar{h}) \geqslant T_{bh})), \\ 1, & \text{otherwise}, \end{cases} \tag{27}$$

$$I_{c1}(c_k) = \begin{cases} 2, & \text{if } ((K_1 = 1) \text{ and } (F(c_k) \geqslant T_1) \\ & \quad \text{and } (A_{\underset{h1}{\sim}}(\bar{h}) \geqslant T_{yh})) \\ & \quad \text{or } ((K_1 = 0) \text{ and } (F(c_k) \geqslant T_1)), \\ 3, & \text{otherwise}. \end{cases} \tag{28}$$

In Eqs. (27) and (28), T_0, T_1, T_{bh}, $T_{yh} \in [0,1]$. T_0 and T_1 are thresholds used to classify, respectively, blue and black as well as yellow and white. Both of them are obtained from the above learning algorithm. K_0 and K_1 are two switch parameters to control color recognition while T_{bh} and T_{yh} are two thresholds set by users when K_0 and K_1 are set to 1. According to the practical situation, we can determine status of the two switch parameters and the corresponding thresholds to change the recognition conditions, thus increasing the flexibility of the algorithm.

After each sub-region's color is identified, the overall confidence levels of two possible colors can be calculated by

$$Z_g(x) = \sum_{k=1}^{N_z} Z_k, \tag{29}$$

where Z_k denotes color confidence level of the kth sub-region. Eq. (29) subjects to $I_c(c_k) = x$ and $Z_k/(W_{R_k} \times H_{R_k}) \geqslant T_p$, where T_p is a pre-defined threshold and $T_p \in [0,1]$. Because of the constraint condition $Z_k/(W_{R_k} \times H_{R_k}) \geqslant T_p$, only those sub-regions whose backgrounds account for the main body are considered during the recognition of R_v's color. Thus it can decrease the influence of character regions on color recognition and improve the algorithm's robustness.

Then R_v's color type can be determined according to the overall confidence levels of possible colors, as described by Eq. (30). And Eq. (31) describes the corresponding confidence level of R_v's color.

$$P_c = \begin{cases} 0, & \text{if } (\xi = 0) \text{ and } (Z_g(0) \geqslant Z_g(1)), \\ 1, & \text{if } (\xi = 0) \text{ and } (Z_g(0) < Z_g(1)), \\ 2, & \text{if } (\xi = 1) \text{ and } (Z_g(2) \geqslant Z_g(3)), \\ 3, & \text{if } (\xi = 1) \text{ and } (Z_g(2) < Z_g(3)). \end{cases} \tag{30}$$

$$Z_p = \arg \max_{x \in \{0,1,2,3\}} (Z_g(x)). \tag{31}$$

Finally, let Z_p^i be color confidence level of the ith valid license plate region. Then the color type of the license plate is identified according to Eq. (32), which means that the color type with the maximal confidence level is the final result.

$$L_c = \arg \max_{i \in \{1,\ldots,N_p\}} (Z_p^i). \tag{32}$$

2.2.3. Summary of the proposed algorithm

Based on the above analysis, the complete algorithmic steps of the fuzzy-based algorithm for color recognition of license plates are summarized as follows:

(1) Accomplish denoising and other pre-processing operations on an input vehicle image that is to be recognized.
(2) Obtain the top N_p candidate license plate regions during the rough localization stage, based on the rank of confidence levels.
(3) For each candidate license plate region, perform steps (4)–(13).
(4) Remove non-plate part from the candidate plate region to obtain the valid plate region, according to Eqs. (1)–(6).
(5) Obtain the reverse color information and classify the license plate into class blue/black or class yellow/white, according to Eq. (7).
(6) Calculate the average gray level of the valid license plate region, according to Eq. (21).
(7) Divide the valid region into some sub-regions, and then re-perform steps (8)–(11) for each sub-region.
(8) Calculate the confidence level and the average YUV information of the sub-region, based on Eqs. (22)–(25).
(9) Convert the average YUV data into the HSV color space, according to Eqs. (8)–(13). Thus obtain the color feature of the sub-region.
(10) Calculate the membership degree of the sub-region's falling into a color type, based on Eqs. (14)–(20).
(11) Identify the sub-region's color type according to Eqs. (26)–(28).
(12) Calculate the overall confidence levels of possible colors of the valid license plate region, based on Eq. (29).
(13) Identify the color type of the valid license plate region and calculate the corresponding confidence level, according to Eqs. (30) and (31), respectively.
(14) Obtain the final color type of the license plate in the input vehicle image, according to Eq. (32).

3. Experimental results and discussion

3.1. Experimental setup

This paper is a sub-model of our DSP-based embedded LPR system, which is run on TI DM642 600 MHz/32 MB RAM and developed with C language under CCStudio V3.1 environment.

For convenience, the proposed algorithm is named FCRA. In order to compare with FCRA, two previous versions of the color recognition algorithm named V1 and V2, as well as some of the traditional classification approaches are adopted in this paper. All algorithms in the experiments perform the color recognition task in the HSV color space. V1 and V2 are thresholds and rules determination methods. For V1, there are 9 thresholds (4 for class yellow/white and 5 for class blue/black) and 6 rules. And there are 40 thresholds (12 for class yellow/white and 28 for class blue/black) and 20 rules within V2. In contrast to V1 and V2, there are 14 thresholds and 12 rules in FCRA. Traditional classification methods include probability-based Bayesian method, distance-based method and Fisher method (Bian et al., 2000). As to distance-based method, vectors composed of hue, saturation and value as well as skewness of Color Moments (Stricker and Orengo, 1995) are used to be the color features, respectively, named Vhsv and CM. And Histogram method (Han and Kamber, 2006) is used to accomplish data reduction and get the representative set of training samples during the training stage. Then NN (Nearest Neighbor) and KNN (K-Nearest Neighbor) methods (Han and Kamber, 2006) are utilized to perform classification task based on distances between samples. During the training stage, we adopted different histograms and parameters to accomplish data reduction: (1) there were three kinds of histograms, namely Equi-Depth, Equi-Width and V-Optimal histograms (Jagadish et al., 1998) and (2) there were three sizes of buckets, namely 10, 20 and 30. While different distance measure functions and parameters were adopted at the recognition stage: (1) two kinds of distance calculation methods, i.e. Euclidean distance and the method of Smith and Chang (1996), were applied and (2) different K-values of KNN were tried, namely 3, 5, 7 and 9. For convenience, results under different methods and parameters are not given here, and only the best results are listed in this paper.

All the above algorithms are evaluated in terms of recall, precision, overall accuracy and overall rejection. Let N_x be the number of vehicle images whose color types of license plates are x. Let N_{rx} be the number of samples that are recognized to be x by recognition algorithms. Let $n_{x\to x}$ refer to the number of images that are classified correctly. Let n_{x0} represent the number of images that have no recognition results. Table 1 shows definitions of the four evaluation indexes.

All test images in the experiments are real scene images that were captured from three cities in Mainland China, Shanghai, Shenzhen and Beijing, with the resolutions of

720×576 (Shanghai) and 768×576 (Shenzhen and Beijing), respectively. The viewing angles of the three sets are different. All the images were taken under different time, weather, lighting and shadowing conditions. And the image quality of Shanghai set is better than those of Shenzhen and Beijing. For comparison convenience, each test set contains the same number of samples while the number of test images for each class is different. In order to validate robustness of the algorithms, there are some plates appeared in various conditions, including partly occluded (named SP1), damaged and degraded seriously (named SP2). The numbers of test images, two main external brightness levels (day and night) and two main special images (SP1 and SP2) for each class are shown in Table 2.

A valid license plate region is divided into 50 sub-regions, i.e. $N_z = 50$. Thresholds of FCRA are mainly learned from the training samples. Based on the priori knowledge about image quality and the number of images for each class, the parameters in Eqs. (27) and (28) are set as follows: (1) Shanghai: $T_0 = 0.60$, $T_1 = 0.40$, $K_0 = 1$, $T_{bh} = 0.95$, $K_1 = 1$, $T_{yh} = 0.90$; (2) Shenzhen: $T_0 = 0.60$, $T_1 = 0.60$, $K_0 = 0$, $K_1 = 1$, $T_{bh} = 0.90$; (3) Beijing: $T_0 = 0.50$, $T_1 = 0.55$, $K_0 = 1$, $T_{bh} = 1.00$, $K_1 = 0$.

3.2. Recognition performances

The color recognition performances of different approaches, in terms of the indexes defined in Table 1, on the above three test sets are shown in Tables 3–5.

In the above Tables, performances of Vhsv are achieved under the following parameters: (1) Shanghai: V-Optimal histogram, 30 buckets, distance of Smith and Chang (1996), and NN method; (2) Shenzhen: Equi-Depth histogram, 30 buckets, distance of Smith and Chang (1996), and 3 votes of KNN and (3) Beijing: V-Optimal histogram, 30 buckets, distance of Smith and Chang (1996), and 7 votes of KNN. Correspondingly, CM's parameters are as follows: (1) Shanghai: V-Optimal histogram, 20 buckets and NN method; (2) Shenzhen: V-Optimal histogram, 20 buckets and 3 votes of KNN and (3) Beijing: V-Optimal histogram, 20 buckets and 9 votes of KNN.

Influenced by many factors, the color feature distributions of samples within class blue/black and class yellow/white overlap frequently. Especially, it is difficult to distinguish between blue and black in some cases. Therefore, color recognition of license plates is not a simple linearly separable problem. And from the above tables, we can also find that great error classification rates are caused by Fisher method, which is a linear classifier.

Because the classification rules and thresholds of V1 and V2 were set specifically for Shanghai based on many experiments, they achieve good performances on Shanghai set. By adding more thresholds and rules while dividing a plate region into 100 sub-regions, V2 improves its performances when it is compared with V1. However, because of lacking learning capability, their performances on Shenzhen and Beijing test sets decrease sharply.

From the above three tables, we can find, in general, that precision rates of black are inferior to those of other license plate types. On the one hand, blue and black are difficult to distinguish under low saturation and illumination conditions. On the other hand, due to the fact that there are much more blue plates than black plates in real situation, black plates in the training sets are less than blue plates. So the learning of blue plates is more sufficient than that of black plates, ensuring the recognition performances of blue plates. Overall, because the number of black plates in Shanghai test set is very small and many vehicle images with black and blue plates are easy to be mixed up, high recall rates and low precision rates are the features of most approaches on black plates. With the increase of black plates in Beijing and Shenzhen sets, recognition performances of black plates increase too. Compared with other approaches, FCRA achieves better performances on black plates.

From Tables 3–5, it can be found that, except Fisher and Vhsv, the overall accuracy rates of other approaches on Shenzhen and Beijing sets are inferior to those on Shanghai set. There are two reasons. Firstly, among the three test sets, the quality of Shanghai is the best and Beijing is the worst. With the decrease of image quality, the overall accuracy rates of these approaches decrease too. Secondly, it can be found from Table 2 that there are more images captured at night in Shenzhen and Beijing than Shanghai, with the proportions of 32.60%, 43.32% and 20.23%, respectively. As to the increase in overall accuracy rates of Fisher and Vhsv instead, it can be explained as follows. From

Table 1
Performance evaluation indexes and their definitions

Index	Definition	Index	Definition
Recall	$\frac{n_{x\to x}}{N_x}$	Precision	$\frac{n_{x\to x}}{N_{rx}}$
Overall accuracy	$\frac{\sum_{x=0}^{3} n_{x\to x}}{\sum_{x=0}^{3} N_x}$	Overall rejection	$\frac{\sum_{x=0}^{3} n_{x0}}{\sum_{x=0}^{3} N_x}$

Table 2
Test sets in the experiments

Test set	Samples	License plate classes				Brightness		Special images	
		Blue	Black	Yellow	White	Day	Night	SP1	SP2
Shanghai	6000	2430	180	2110	1280	4786	1214	150	171
Shenzhen	6000	3237	946	1205	612	4044	1956	98	77
Beijing	6000	3350	426	899	1325	3401	2599	273	199

Table 3
Color recognition performances of different approaches on Shanghai test set

Performance	Fisher	Vhsv	V1	Bayesian	V2	CM	FACR
Blue							
Recall rate (%)	53.25	81.19	93.46	93.79	97.45	96.26	97.04
Precision rate (%)	99.85	99.80	97.72	98.66	94.95	97.62	96.60
Black							
Recall rate (%)	98.33	97.22	73.33	86.11	34.44	70.56	56.11
Precision rate (%)	13.68	28.55	49.44	54.39	63.92	65.46	67.79
Yellow							
Recall rate (%)	94.22	95.64	95.69	95.07	95.69	95.88	95.69
Precision rate (%)	100.00	100.00	99.36	98.48	100.00	98.92	99.95
White							
Recall rate (%)	99.45	99.45	98.44	97.27	99.53	97.73	99.38
Precision rate (%)	94.72	97.03	97.30	95.92	97.10	97.35	97.03
Overall rejection rate (%)	01.30	01.33	01.37	01.17	01.30	01.33	01.32
Overall accuracy rate (%)	78.87	90.65	94.70	94.75	95.38	95.67	95.83

Table 4
Color recognition performances of different approaches on Shenzhen test set

Performance	V1	Fisher	V2	Bayesian	Vhsv	CM	FACR
Blue							
Recall rate (%)	96.35	77.63	97.62	98.49	95.74	95.83	97.16
Precision rate (%)	84.71	97.74	84.11	92.19	94.65	95.77	95.51
Black							
Recall rate (%)	39.53	92.81	35.84	71.04	80.44	84.46	83.30
Precision rate (%)	78.90	55.43	85.18	95.59	86.38	87.23	91.42
Yellow							
Recall rate (%)	96.93	88.13	96.43	95.60	94.19	94.27	96.51
Precision rate (%)	83.37	99.81	87.37	94.19	99.65	99.56	97.65
White							
Recall rate (%)	60.62	99.51	71.24	88.89	99.18	99.02	95.26
Precision rate (%)	93.45	80.34	91.40	91.28	88.87	88.99	92.69
Overall rejection rate (%)	00.77	00.38	00.63	00.33	00.38	00.38	00.42
Overall accuracy rate (%)	83.87	84.37	84.95	92.60	93.37	94.05	94.65

Table 5
Color recognition performances of different approaches on Beijing test set

Performance	V1	V2	Fisher	Vhsv	CM	Bayesian	FACR
Blue							
Recall rate (%)	80.60	83.49	71.67	93.43	94.75	93.10	94.99
Precision rate (%)	93.14	92.65	99.21	93.80	93.19	96.27	95.58
Black							
Recall rate (%)	55.63	50.23	96.01	51.17	45.77	72.77	66.20
Precision rate (%)	29.59	31.42	31.95	60.22	66.55	67.54	76.22
Yellow							
Recall rate (%)	92.10	91.43	90.88	91.10	91.21	90.99	90.77
Precision rate (%)	53.98	59.01	93.37	99.64	99.39	98.44	99.63
White							
Recall rate (%)	46.72	56.68	95.17	99.32	99.17	98.64	99.32
Precision rate (%)	97.48	97.15	97.45	97.63	97.70	97.54	97.41
Overall rejection rate (%)	02.18	02.23	02.18	02.18	02.18	02.17	02.18
Overall accuracy rate (%)	73.07	76.40	81.47	91.38	91.72	92.57	93.27

Table 2, it is clear that there are more blue and black plates in Shenzhen and Beijing while there are more yellow and white plates in Shanghai. For all approaches in Shenzhen and Beijing, the total number of blue and black plates whose colors were recognized correctly increased while the total number of yellow and white plates classified correctly decreased. For Fisher and Vhsv, the total increment was greater than the total decrement. But for other approaches, it was the opposite situation. Therefore, the overall accuracy rates of Fisher and Vhsv increased.

Among the images that were not recognized correctly by FCRA, most of them occurred during the localization stage. Because of the influence of English brands, vehicle lights and some other fake regions whose structure and texture were similar to vehicle plates, these images' plate regions were not located correctly. In particular, because of camera distortion, some of them in Shenzhen and Beijing test sets were difficult to distinguish. Some others were under low saturation and dark conditions, thus they themselves were easy to be mixed up.

As to the images that had no recognition results, they occurred when vehicle lights were too strong at night, the illumination was too low and license plates were degraded or occluded seriously. These images were rejected because the system failed to detect plate regions during the localization stage or because of low confidence level during the recognition stage.

For FCRA, if the switch parameters in Eqs. (27) and (28) were set to 0 and there was no sub-region division operation, its overall accuracy rates would be 95.05% on Shanghai, 92.17% on Shenzhen and 93.23% on Beijing, respectively. From the experiments, we can notice that FCRA achieves the best results on the above three test sets, compared with other approaches. Obviously, the recognition accuracy and adaptability are improved through the introduction of fuzzy logic and integration with a learning algorithm. Therefore, it is helpful to improve the final performance of license plate recognition.

3.3. Recognition time

For comparison convenience, we take the average recognition time of the whole license plates to evaluate the computational costs of all color recognition algorithms indirectly. It includes the execution time to finish all the steps, i.e. pre-processing, plate localization, color recognition, character separation and model matching. On the other hand, it can be found from Fig. 1 that a white plate may have several different formats. In general, it costs much more time to recognize a vehicle image with white plate, compared with the other three types. From Table 2, we find that the numbers of samples for each type are different in the above test sets. For comparison justice, we choose the same number of samples for each type from the above sets to constitute the new test sets, where there are 4121 samples consisted of 2430 blue, 180 black, 899 yellow and 612 white plates. After all images in a test set are recognized, the mean value is then treated as the average recognition time. The optimization option of the compiler is set to −O2.

Furthermore, if the system fails to locate a license plate in a vehicle image, sometimes it will not perform some operations, such as color recognition, character separation and model matching. And its execution time may be much less than that of the normal recognition process. To avoid the influence of such samples, their execution time is not taken into consideration in the experiments. The results are shown in Table 6.

From Table 6, it can be found that CM and Vhsv approaches cost much more time than other approaches, because they are based on KNN algorithm that has to compare with many training samples during the recognition process. For Vhsv, it needs to calculate trigonometric function when it compares the similarity between two colors, by the method of Smith and Chang (1996). Thus it is the most computationally expensive approach on the three test sets, without further optimization.

For all the approaches, it is clear that the average recognition time in Shanghai is less than that in Shenzhen and Beijing, because of lower image resolution. Although the image resolutions of Shenzhen and Beijing are the same one, the average recognition time in Shenzhen is greater than that in Beijing. It is because there are much more images captured at night in the new Beijing set than those in Shenzhen, where the numbers are 912 and 236, respectively. For images at night in Beijing, it is very common that only the regions of license plates and vehicle lights are clear. But the images at night in Shenzhen are more complex. Fig. 8 gives such two examples. Obviously, the system needs to spend more time performing plate localization task. Let us take the two images in Fig. 8 for example. FCRA cost, respectively, 433 ms and 376 ms to recognize image (a) and (b), where the localization time is 156 ms and 96 ms, respectively.

For Vhsv approach, it can also be found from Table 6 that the difference of average recognition time between Shenzhen and Beijing is not so obvious as other approaches. It is caused by those images whose execution time was not taken into account. From the statistic information about those time records, we found that their average execution time in Shenzhen was greater than that in Beijing. When those time records were removed, the average increments in Shenzhen were less than those in Beijing. For Vhsv, the difference between the two average increments was 10.42 ms, which was greater than all the other approaches (less than 6 ms). Thus, for Vhsv, the difference of average recognition time between the two tests became small.

To sum up, the proposed algorithm achieves better recognition performances in three test sets. While it does not increase the computational cost of LPR and can meet the real-time requirement of the practical engineering applications.

Table 6
Average recognition time of the whole license plates (ms)

Test set	V1	Bayesian	V2	FACR	Fisher	CM	Vhsv
Shanghai	395.36	395.45	395.65	395.99	397.17	501.21	975.24
Shenzhen	437.70	442.59	438.59	444.40	447.02	576.32	1136.39
Beijing	405.94	412.64	406.42	412.14	412.23	556.72	1135.98

Fig. 8. Two examples of vehicle images captured at night: (a) blue plate of Shenzhen and (b) blue plate of Beijing.

4. Conclusions and future works

Considering LPR works under various scenes and complex conditions, this paper presents a new algorithm for color recognition of license plates. Through the introduction of fuzzy logic in the HSV color space and integration with a learning algorithm, the accuracy and adaptability of the proposed algorithm are improved. Comparison experiments with some other color recognition algorithms and classification methods demonstrate that the proposed algorithm can accomplish the color recognition task for license plates effectively and efficiently. Both of the recognition accuracy and execution time can meet the requirements of the practical engineering applications.

From the experiments, we found that most of the images that were not recognized correctly were caused by wrong localization, influenced by English brands, vehicle lights and some other fake regions whose structure and texture were similar to vehicle plates, and camera distortion. Therefore, our future works will focus on improving precision of the localization algorithm and developing a better camera control algorithm. Meanwhile, further optimization of the program to improve its efficiency is also our concern.

Acknowledgements

This work has been supported by Sichuan University Wisesoft Software Co. Ltd. The authors thank the web site http://www.fourcc.org/ for Julien's equations of YUV to RGB conversion, and http://www.mathcs.emory.edu/~cheung/Courses/584-StreamDB/Syllabus/06-Histograms/ for the documents and primitive source code about V-Optimal histogram approach.

References

Berwick, D., Lee, S.W., 2004. Spectral gradients for color-based object recognition and indexing. Computer Vision and Image Understanding 94, 28–43.

Bian, Z.Q., Zhang, X.G., et al., 2000. Pattern Recognition, second ed. Tsinghua University Press, Beijing (in Chinese).

Buluswar, S.D., Draper, B.A., 1998. Color recognition in outdoor images. In: Proc. 6th Internat. Conf. on Computer Vision, Bombay, India, pp. 171–177.

Chen, C.L., Wu, W.J., 2005. Color pattern recognition with the multichannel non-zero-order joint transform correlator based on the HSV color space. Optics Comm. 244, 51–59.

Drew, M.S., Wei, J., Li, Z.N., 1998. On illumination invariance in color object recognition. Pattern Recognition 31 (8), 1077–1087.

Finlayson, G., Xu, R.X., 2003. Illuminant and gamma comprehensive normalisation in logRGB space. Pattern Recognition Lett. 24, 1679–1690.

Fu, Y.P., Li, Z.N., Yuan, D., 2004. Improving license plate recognition system by color algorithms based on HIS space. J. Computer Eng. Des. 25 (5), 703–707 (in Chinese).

Funt, B.V., Finlayson, G.D., 1995. Color constant color indexing. IEEE Trans. Pattern Anal. Machine Intell. 17 (5), 522–529.

Geske, G., Stupmann, F., Wego, A., 2003. High speed color recognition with an analog neural network chip. In: Proc. IEEE Internat. Conf. on Industrial Technology, Maribor, Slovenia, pp. 104–107.

Gevers, T., Smeulders, A.W.M., 1999. Color-based object recognition. Pattern Recognition 32, 453–464.

Han, J.W., Kamber, M., 2006. Data Mining: Concepts and Techniques, second ed. China Machine Press, Beijing (Chinese edition).

Huang, J., Kumar, S.R., Mitra, M., et al., 1997. Image indexing using color correlograms. In: Proc. IEEE Internat. Conf. on Computer Vision and Pattern Recognition, San Juan, PuertoRico, pp. 762–768.

Jagadish, H.V., Koudas, N., Muthukrishnan, S., et al., 1998. Optimal histograms with quality guarantees. In: Proc. 24th Internat. Conf. on Very Large Data Bases, New York, USA, pp. 275–286.

Lalanne, T., Lempereur, C., 1998. Color recognition with a camera: a supervised algorithm for classification. In: Proc. IEEE Southwest Symposium on Image Analysis and Interpretation, Tucson, USA, pp. 198–204.

Lin, Z.Y., Wang, J.X., Ma, K.K., 2002. Using eigencolor normalization for illumination-invariant color object recognition. Pattern Recognition 35, 2629–2642.

Makoto, M., Yasuhiro, Y., 1988. Mathematical transform of (R,G,B) color data to Munsell (H,V,C) color data. In: Proc. Visual Communications and Image Processing, Massachusetts, USA, pp. 650–657.

Parkkinen, J., Oja, E., Jaaskelainen, T., 1988. Color analysis by learning subspaces and optical processing. In: Proc. IEEE Internat. Conf. on Neural Networks, San Diego, USA, pp. 421–427.

Pavlova, P.E., Cyrrilov, K.P., Moumdjiev, I.N., 1996. Application of HSV color system in identification by color of biological objects on the basis of microscopic images. Comput. Med. Imaging Graphics 20 (5), 357–364.

Smith, J.R., Chang, S.F., 1996. VisualSEEk: A fully automated content-based image query system. In: Proc. ACM Multimedia, Boston, USA, pp. 87–98.

Smith, J.R., Chang, S.F., 1997. Visually searching the web for content. IEEE Trans. Multimedia 4 (3), 12–20.

Stachowicz, M.S., Lemke, D., 2000. Color recognition. In: Proc. 22nd Internat. Conf. on Information Technology Interfaces, Pula, Croatia, pp. 329–334.

Stricker, M., Orengo, M., 1995. Similarity of color images. In: Proc. SPIE Conf. on Storage and Retrieval for Image and Video Databases III, San Jose, USA, pp. 381–392.

Swain, M.J., Ballard, D.H., 1991. Color indexing. Int. J. Comput. Vision 7 (1), 11–32.

Tao, L.M., Xu, G.Y., 2001. Color in machine vision and its application. Chin. Sci. Bull. 46 (17), 1411–1421.

Tsin, Y.H., Collins, R.T., Ramesh, V., et al., 2001. Bayesian color constancy for outdoor object recognition. In: IEEE Conf. on Computer Vision and Pattern Recognition, Kauai, USA, pp. I-1132–I-1139.

Vertan, C., Boujemaa, N., 2000. Using fuzzy histograms and distances for color image retrieval. In: Proc. Challenge of Image Retrieval, Brighton, UK, pp.1–6.

Vitabile, S., Pollaccia, G., Pilato, G., et al., 2001. Road signs recognition using a dynamic pixel aggregation technique in the HSV color space. In: Proc. 11th Internat. Conf. on Image Analysis and Processing, Palermo, Italy, pp. 572–577.

Wang, X.L., Zhou, M.Q., Geng, G.H., 2004. An approach of vehicle plate extract based on HSV color space. J. Comput. Eng. 30 (17), 133–135 (in Chinese).

Xu, J.F., Li, S.F., Chen, Z.B., 2003. Color analysis for Chinese car plate recognition. In: Proc. IEEE Internat. Conf. on Robotics, Intelligent Systems and Signal Processing, Changsha, China, pp. 1312–1316.

Yang, J.H., Wang, J.Y., 2004. A method for locating the license plate based on color segmentation and shape-texture analysis. J. Transport. Eng. Infor. 12 (1), 99–105 (in Chinese).

Yang, Y.Q., Bai, J., Tian, R.L., et al., 2005. A vehicle license plate recognition system based on fixed color collocation. In: Proc. 4th Internat. Conf. on Machine Learning and Cybernetics, Guangzhou, China, pp. 5394–5397.

Zhai, H.C., Chavel, P., Wang, Y., et al., 2005. Weighted fuzzy correlation for similarity measure of color-histograms. Optics Comm. 247, 49–55.